ORIGINAL ARTICLE

Model of persistent foot-and-mouth disease virus infection in multilayered cells derived from bovine dorsal soft palate

Sara Hägglund[1] | Eve Laloy[2] | Katarina Näslund[1] | Florian Pfaff[3] |
Michael Eschbaumer[3] | Aurore Romey[2] | Anthony Relmy[2] | Annika Rikberg[1] |
Anna Svensson[1] | Helene Huet[2] | Kamila Gorna[2] | Daniela Zühlke[4] |
Katharina Riedel[4] | Martin Beer[3] | Stephan Zientara[2] | Labib Bakkali-Kassimi[2] |
Sandra Blaise-Boisseau[2] | Jean François Valarcher[1]

[1]Host Pathogen Interaction Group, Section of Ruminant Medicine, Department of Clinical Science, Swedish University of Agricultural Sciences (SLU), Uppsala, Sweden

[2]Laboratoire de Santé Animale de Maisons-Alfort, UMR 1161 virologie, INRA, Ecole Nationale Vétérinaire d'Alfort, ANSES, Université Paris-Est, Maisons-Alfort, France

[3]Institute of Diagnostic Virology, Friedrich-Loeffler-Institut, Greifswald-Insel Riems, Germany

[4]Institute of Microbiology, Department for Microbial Physiology and Molecular Biology, University of Greifswald, Greifswald, Germany

Correspondence
Jean François Valarcher, Host Pathogen Interaction Group, Section of Ruminant Medicine, Dept. of Clinical Science, Swedish University of Agricultural Sciences (SLU), Ulls väg 26, 75007 Uppsala, Sweden.
Email: jean-francois.valarcher@slu.se

Funding information
Svenska Forskningsrådet Formas; Federal Office for Agriculture and Food (BLE, Germany); Agence Nationale de la Recherche, Grant/Award Number: ANIHWA ERA NET Transcriptovac FP#26

Abstract

Foot-and-mouth disease virus (FMDV) causes a highly contagious vesicular disease in livestock, with serious consequences for international trade. The virus persists in the nasopharynx of cattle and this slows down the process to obtain an FMDV-free status after an outbreak. To study biological mechanisms, or to identify molecules that can be targeted to diagnose or interfere with persistence, we developed a model of persistent FMDV infection in bovine dorsal soft palate (DSP). Primary DSP cells were isolated after commercial slaughter and were cultured in multilayers at the air-liquid interface. After 5 weeks of culture without further passage, the cells were infected with FMDV strain O/FRA/1/2001. Approximately, 20% of cells still had a polygonal morphology and displayed tight junctions as in stratified squamous epithelia. Subsets of cells expressed cytokeratin and most or all cells expressed vimentin. In contrast to monolayers in medium, multilayers in air demonstrated only a limited cytopathic effect. Integrin $\alpha_V\beta_6$ expression was observed in mono- but not in multilayers. FMDV antigen, FMDV RNA and live virus were detected from day 1 to 28, with peaks at day 1 and 2. The proportion of infected cells was highest at 24 hr (3% and 36% of cells at an MOI of 0.01 and 1, respectively). At day 28 after infection, at a time when animals that still harbour FMDV are considered carriers, FMDV antigen was detected in 0.2%–2.1% of cells, in all layers, and live virus was isolated from supernatants of 6/8 cultures. On the consensus level, the viral genome did not change within the first 24 hr after infection. Only a few minor single nucleotide variants were detected, giving no indication of the presence of a viral quasispecies. The air-liquid interface model of DSP brings new possibilities to investigate FMDV persistence in a controlled manner.

Hägglund, Laloy, Näslund, Blaise-Boisseau equally contributed to this work.

1 | INTRODUCTION

Foot-and-mouth disease (FMD), a highly contagious vesicular disease of cloven-hoofed animals, has important consequences for livestock farming. FMD influences the agricultural economy on a global scale, partly by affecting production (Rweyemamu et al., 2008), but also because a country's official FMD status determines its access to international markets (OIE, 2018). A confirmed FMD diagnosis can result in exclusion from the most profitable trade (Knight-Jones & Rushton, 2013). The aetiologic agent of FMD is a 30 nm sized, positive-sensed single-stranded RNA virus, the FMD virus (FMDV), which belongs to the genus *Aphthovirus* within the family *Picornaviridae*. The FMD virions consist of naked capsids with high antigenic variation, resulting in the existence of seven serotypes (O, A, C, SAT1, SAT2, SAT3 and Asia 1) and multiple subtypes. Both domesticated and wild even-toed ungulates can become infected. In cattle, the clinical signs are characterized by vesicular lesions in and around the mouth, on the muzzle, feet and udder, and by sudden deaths in young individuals, as well as by secondary affections such as mastitis and reproductive disturbances (Kitching, 2002). Virus shedding occurs already before clinical signs, which, in combination with high viral loads and high level of tenacity in the environment, leads to a very high transmissibility (Alexandersen, Quan, Murphy, Knight, & Zhang, 2003; Bravo de Rueda, de Jong, Eble, & Dekker, 2015). Moreover, infected cattle can carry virus in the pharyngeal area for a prolonged period, even despite preceding vaccination (Eschbaumer et al., 2016; Stenfeldt et al., 2016). Animals that harbour FMDV longer than 28 days post-infection (dpi) are defined as carriers (OIE, 2018) and, although convincing scientific evidence for spontaneous virus transmission to naïve animals is missing (Bertram et al., 2018; Bronsvoort et al., 2016; Maree et al., 2016; Parthiban, Mahapatra, Gubbins, & Parida, 2015), carriers are considered a potential virus source, either in vivo or post-mortem (Arzt, Belsham, Lohse, Botner, & Stenfeldt, 2018). This slows down the process to return to the status 'FMD free country or zone' and favours stamping-out strategies for disease control following an incursion of the virus. Persistent virus replicates in follicle-associated epithelium in the nasopharynx and soft palate (Alexandersen, Zhang, & Donaldson, 2002; Arzt, Juleff, Zhang, & Rodriguez, 2011; Stenfeldt et al., 2016) and is stored in an inactive form in the germinal centres of nasopharyngeal lymph nodes (Juleff et al., 2008; Maree et al., 2016). Reliable diagnostic methods to identify the persistently infected animals are lacking. Repeated oropharyngeal probang sampling or pharyngeal tonsil swabs are needed (Maree et al., 2016) and the probability to detect a carrier cattle in a herd rapidly decreases, both with time after an outbreak and with the age of the sampled animal (Bronsvoort et al., 2016). More robust ways to diagnose persistence, or even to treat or

prevent this condition, could potentially help in the control of FMDV. However, to reach these goals, the mechanisms involved need to be elucidated.

Suggestions have already been put forward on how persistence is induced, such as through viral suppression of host immune responses (Pacheco et al., 2015; Stenfeldt et al., 2016; Stenfeldt, Eschbaumer, et al., 2017), adaptation of host cells to the virus (Martin Hernandez, Carrillo, Sevilla, & Domingo, 1994; de la Torre et al., 1988) or vice versa, through mutations in the viral genome leading to functional changes, such as immune escape (Gebauer et al., 1988), or a change in the use of receptors (O'Donnell et al., 2014). Studies have been performed in animals as well as in monolayers of pharyngeal cells or other epithelial cell lines, namely BHK-1, IBRS-2 and MDBK cells (Kopliku et al., 2015; O'Donnell et al., 2014; de la Torre, Davila, Sobrino, Ortin, & Domingo, 1985). The drawback of cells in culture is that they need to be regularly disrupted, that is passaged, in order to survive. To avoid such passages, which do not occur in vivo, we developed a model of multilayer cells from the dorsal soft palate (DSP) that can be left intact for several months. The aim was to establish a model of persistent infection, to enable future studies of virus-host interactions, or the screening of molecules to detect or interfere in persistence. Hypotheses raised from results obtained in this model could be verified in live animals and, hopefully in routine, in vitro studies in the model could precede interventional in vivo studies to spare experimental animals.

2 | MATERIALS AND METHODS

2.1 | Virus

The FMDV O Clone 2.2 (Cl 2.2) used in this study is a twice-plaque-purified viral clone derived from the O/FRA/1/2001 strain (Kopliku et al., 2015) that was further propagated on BHK-21 cells (four passages). Viral batches were titrated on BHK-21 monolayers by plaque assay as described in Kopliku et al., (2015).

2.2 | Isolation of cells from the bovine dorsal soft palate

Epithelial tissue from the DSP was collected immediately after commercial slaughter of clinically healthy, conventionally reared adult male and female cattle of the Swedish red and white breed. During transport to the laboratory, the tissue was stored in incubation medium consisting of Dulbecco's Modified Eagle's Medium (DMEM, Lonza, Belgium), supplemented per litre with 2.5 mg amphotericin B (Sigma-Aldrich, A-9528), 1 mg deoxyribonuclease (Sigma-Aldrich, DN-25), 1 g dithiothreitol (Sigma-Aldrich, D-0632), 20 mg gentamicin

(Sigma-Aldrich, G-1397), 20 ml 1 M HEPES (VWR, BioWhittaker BE17-737F), 10 ml 200 mM L-glutamine (VWR, BioWhittaker BE17-605F), 60 mg penicillin G sodium salt (Sigma-Aldrich, P3032) and 100 mg streptomycin sulphate salt (Sigma-Aldrich, S6501). In the laboratory, epithelial tissue was dissected and digested at 4°C overnight in incubation medium additionally supplemented per litre with 1 g protease XIV (Sigma-Aldrich, P5147).

Epithelial cells were thereafter manually scraped off the underlying tissue, filtered through a 40 μm cell strainer and incubated in cell culture flasks for 4 hr at 37°C and 5% CO_2. At this stage, the cell culture medium consisted of DMEM containing 10% gamma-irradiated, heat inactivated, foetal calf sera (FCS, Hyclone™, GE Healthcare) and supplemented per litre with 31.25 KU Nystatin (Sigma-Aldrich, N6261), in addition to HEPES, L-glutamin, penicillin G and streptomycin as above.

Cells that did not adhere to the plastic were centrifuged at 200× g for 10 min at room temperature. They were thereafter frozen, thawed and propagated for three to five passages in cell culture flasks before being seeded in 12 mm diameter Corning® Transwell®-COL collagen-coated PTFE membrane inserts with 3.0 μm pores (Sigma-Aldrich, CLS3494, Figure 1) at a density of 7.5×10^5 cells per insert. The cell culture medium was DMEM/ Nutrient Mixture F-12 Ham (Sigma-Aldrich, D8437), containing 10% FCS and supplemented per litre with 20 μg recombinant human hepatocyte growth factor (Sigma-Aldrich, H9661), in addition to L-glutamine, penicillin G and streptomycin as above. This medium was removed from the upper compartment after five days of culture and changed in the lower compartment every two or three days (Figure 1).

2.3 | Cell characterization

The cellular expression of cytokeratin, integrin $\alpha_v\beta_6$ and vimentin was analysed after freezing and thawing of the cells, and after three to five passages in flasks and culture in a Nunc®Lab-Tek® permanox Chamber Slide™ system (Sigma-Aldrich, C7182), as well as in cells cultured in multilayers on inserts at the air-liquid interphase for five weeks without passage. Cells were fixed in –20°C methanol for 5 min at room temperature prior to staining. The target molecules were detected by immunofluorescence microscopy (in a Nikon Eclipse Ts2R microscope) or co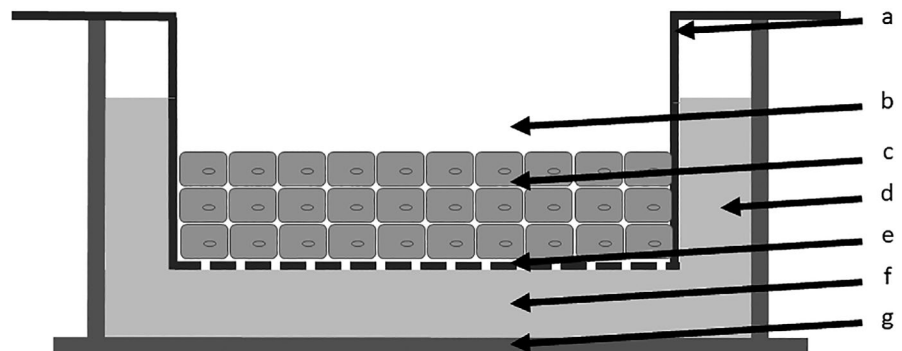nfocal laser scan microscopy (in a ZEISS LSM700 microscope) by using mouse monoclonal antibodies against human cytokeratin (type 4, 5, 6, 8, 10, 13 and 18, clone C-11, Sigma-Aldrich, C2931, with interspecies cross-reactivity) and bovine vimentin (clone RV202, Santa Cruz Biotech, sc-32322) and mouse integrin $\alpha_v\beta_6$ (clone 10D5, Abcam, ab77906 (Burman et al., 2006), together with rat monoclonal antibodies against mouse IgG_1 or IgG_{2a} heavy chain, conjugated with FITC or Alexa 647, respectively (clone M1-14D12, eBioscience, 11-4015, or clone SB84a, Abcam, ab172325, respectively). The cells were mounted with ProLong® Diamond Antifade Mountant with DAPI (Life technologies corporation), according to the manufacturer's instructions. The cytokeratin expression was further assessed by immunohistochemistry (IHC) on paraffin-embedded, FMDV-infected inserts with a pan-cytokeratin cocktail that consisted of two monoclonal mouse antibodies (clones A1/A3, DAKO, M3515, which recognize cytokeratin 1, 2, 3, 4, 5, 6, 7, 8, 10, 13, 14, 15, 16 and 19 and which recognized bovine epithelial cells). Immunohistochemistry (IHC) was performed using an automated Discovery XT (Ventana Medical Systems, Roche Diagnostics), with streptavidin-biotin-alkaline phosphatase, 5-bromo-4-chloro-3-indolyl phosphate as a substrate and nuclear fast red counterstaining.

The cell morphology was studied by light and electron microscopy. For light microscopy, after fixation in 10% buffered formalin, selected multilayers and the underlying PTFE membranes were embedded in 1.3% agarose then left in 70% ethanol overnight. They were then embedded in paraffin, routinely processed, sliced at 4 μm, stained with haematoxylin-eosin-saffron (HES) and examined by light microscopy. For electron microscopy, two control multilayers and the underlying PTFE membrane were fixed in Sörensen phosphate buffer containing 2.5% glutaraldehyde, 0.1% picric acid, 2% paraformaldehyde and 0.18 mol/L sucrose. The samples were postfixed in 1% osmium tetroxide then washed in Sörensen buffer. They were then dehydrated in ethanol and embedded in Spürr's low viscosity epoxy resin. Semi-thin sections were stained with Toluidine blue for light microscopy. Ultra-thin sections (60 nm) were stained with uranyl acetate and examined under a Hitachi-7100 transmission electron microscope equipped with a digital camera.

2.4 | Experimental design and FMDV infection

Dorsal SP cells were cultured on inserts for five weeks and were thereafter infected with FMDV O Cl 2.2, or a placebo. In the first

FIGURE 1 Schematic draw of a permeable insert used to propagate multilayers of bovine dorsal soft palate cells. Insert (a); upper compartment (b); multilayer of bovine dorsal soft palate cells (c); cell culture medium (d); porous membrane (e); lower compartment (f) and well (g) of a 12-well plate

and second experiment (Exp 1 and 2), cells originated from a male and a female, respectively, and were infected at a multiplicity of infection (MOI) of 0.01. In a third experiment (Exp 3), the cells originated from the same female individual as in Exp 2, but were infected at an MOI of 1. A different batch of virus (albeit from the same passage) was used in Exp 1, compared to Exp 2 and 3, which were performed with the same batch. The inserts were incubated for 1 hr with 500 µl of cell lysate from FMDV-infected or uninfected cell cultures that had been clarified by centrifugation. The inoculum was then left on the inserts (Exp 1 and 2) or removed (Exp 3). Immediately following infection and thereafter at a maximum interval of three days, the upper compartments were washed with 500 µl cell culture medium containing 10% FCS and, similarly, but only from 2 dpi, the medium in the lower compartments was changed (for the compartment layout and experimental design, please see Figures 1 and 2, respectively). The wash medium was harvested and frozen at −80°C, pure and diluted 1:4 in TRIzol LS (Invitrogen), for assays of infectious FMDV and FMDV RNA, respectively, as indicated in Figure 2. Moreover, inserts were regularly harvested and fixed, embedded and then cross-sectioned for the detection of FMDV antigens, until day 28 (Figure 2). Cells from 0, 1 and 28 dpi were lysed in TRIzol and stored at −80°C for viral RNA sequencing and for transcriptome analyses. In total, 90 inserts were used in the study.

2.5 | FMDV isolation

2.5.1 | Cell line

IBRS-2 swine kidney epithelial cells (CCLV-RIE 103, FLI) were grown in Earle's minimum essential medium (MEM) with L-glutamine (Invitrogen), supplemented with 7% FCS (Eurobio, Courtaboeuf, France), 1.5% lactalbumin hydrolysate (Sigma-Aldrich), 1% penicillin-streptomycin (PS) (Invitrogen) and 25 mM HEPES (Invitrogen).

2.5.2 | Assessment of FMDV-infectivity

Samples of undiluted cell culture medium used to wash the upper compartments of the inserts were analysed for infectious virus. Ninety-six-well plates were seeded with 5 x 10^4 IBRS-2 cells per well and incubated at 37°C under 5% CO_2 for 24 hr. The monolayers were thereafter washed twice with serum-free culture medium and each sample from the DSP cultures was inoculated in a volume of 50 µl per well. After 1 hr of adsorption at 37°C under 5% CO_2, 250 µl of growth medium was added. Cells were then incubated at 37°C under 5% CO_2 and were monitored for cytopathic effect (CPE) for 48 hr. Immunofluorescent detection was performed using monoclonal antibodies raised against the capsid protein VP2 of FMDV type O (mAb 13G11), as described in Kopliku et al., 2015.

Virus titrations were performed on diluted wash-samples (from 1:10). Fifty µl of cell culture medium without serum was added in each well of 96-well plates. Ten-fold serial dilutions of virus (50 µl per well, eight replicates per dilution) were distributed, and the same volume of growth medium was added to the mock-infected control wells. About 50 µl of IBRS-2 cell suspension at 3 × 10^5 cells/ml in medium was added in each well. Plates were incubated at 37°C under 5% CO_2. Three dpi, plates were fixed with 70% ethanol for 30 min at room temperature (RT) and then stained with methylene blue (1% w/v in water). Values for 50% tissue culture infective dose ($TCID_{50}$) per 50 µl were calculated using the Stellmann and Bornarel table (Stellmann & Bornarel, 1971) and were translated into values per ml.

2.6 | Detection of FMDV RNA

2.6.1 | RNA extraction for FMDV RT-qPCR

Viral RNA was extracted from 50 µl of cell culture washes from the upper compartment, using the LSI MagVet Universal Isolation kit (Life Technologies SAS) and a KingFisher robotic magnetic particle processor (Thermo Scientific) according to the manufacturers' instructions. In total, 2–6 samples were analysed per time point,
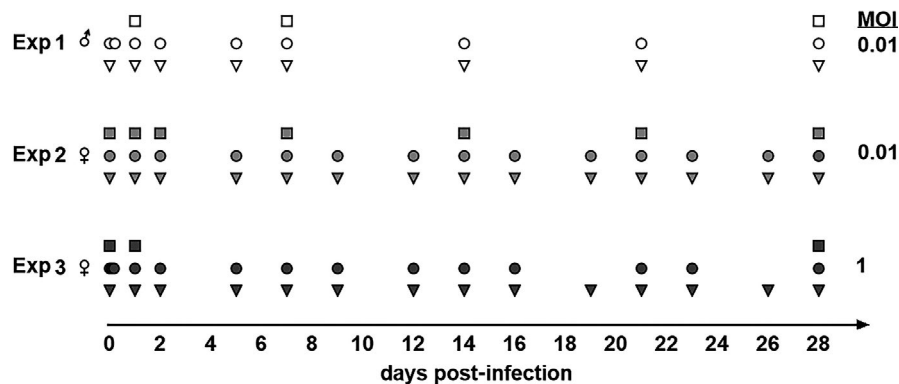

FIGURE 2 Experiment timeline and FMDV detection. Bovine dorsal soft palate cells were propagated in multilayers on porous membrane inserts in the air-liquid interphase and were infected with FMDV O Cl2.2, or placebo. In experiment 1 (Exp 1, empty legends) and 2 (Exp 2, light grey legends), cells derived from male and female cattle, respectively, and were infected at an MOI of 0.01. In experiment 3 (Exp 3, dark grey legends) cells derived from the same female cattle and were infected at an MOI of 1. Cell culture medium and cells were analysed for the presence of FMDV, by virus isolation (triangles), RT-qPCR (circles) or immunohistochemistry (squares), at indicated days post-infection

except for in experiment 3, when single samples were analysed at 2 and 4 hr post-infection (hpi), as well as at 5, 7, 12, 16 and 23 dpi. The RNAs were eluted with 80 μl of elution buffer provided with the kit.

2.6.2 | One-step duplex real-time FMDV RT-qPCR

A one-step duplex pan-FMDV real-time RT-PCR (rtRT-PCR) assay was used as previously described (Gorna et al., 2016). The assay targeted the FMDV 3D coding region and the cellular β-actin gene as an internal control. A weakly positive FMDV RNA control was included in each run as well as a negative control containing water only.

2.7 | Detection of FMDV antigen by immunohistochemistry

Immunohistochemistry was performed using an automated Discovery XT (Ventana Medical Systems, Roche Diagnostics), with streptavidin-biotin-peroxidase, 3′-diaminobenzidine as a substrate and haematoxylin counterstaining. The primary antibodies were rabbit polyclonal against FMDV (FMDV O1 Manisa R3 262/97, The Pirbright Institute, United Kingdom) used at 1/1000; mouse monoclonal against FMDV non-structural protein 3D polymerase (mAb 3F12, kindly provided by Dr E. Brocchi from IZSLER, Brescia, Italy) and mouse monoclonal against cytokeratin AE1-AE3 (M3515, DAKO), used at 1/500.

Positivity for FMDV was evaluated by image analysis of sections stained with polyclonal antibodies. Scanned images of two sections per insert were taken by an ImagerZ1 Zeiss microscope and an AxioCam HRc Zeiss camera. FMDV-positive cells and total number of cells (mean 600, SD 306 cells per insert) were manually counted on each section with ImageJ Cell Counter (Schneider, Rasband, & Eliceiri, 2012).

2.8 | FMDV genome analysis, proteomics and transcriptomics

2.8.1 | RNA extraction and sequencing

For further cell characterization and for sequencing of the FMDV inoculum strain, total RNA was extracted from FMDV O Cl 2.2 and libraries were prepared as described in Pfaff et al., (2018). Briefly, total RNA was extracted from cell culture supernatant using TRIzol (Life Technologies) in combination with the RNeasy Mini Kit (Qiagen, Hilden, Germany). Double-stranded cDNA was generated using the cDNA synthesis system kit (Roche) together with random hexamer primers (Roche). Subsequently, the GeneRead DNA Library L Core Kit (Qiagen) was used to prepare libraries for sequencing on the Ion S5XL system using the Ion 530 OT2 and Chip kit (Life Technologies). For sequencing of FMDV from inserts, polyadenylated RNA was used as described previously (Pfaff et al., 2019) from infected cell lysates obtained at 24 hpi and 28 dpi in Exp 1 and 2. Briefly, total RNA was extracted as described above and mRNA was enriched using the Dynabeads mRNA DIRECT Micro kit (Invitrogen). Subsequently,

whole-transcriptome libraries were prepared using the Ion Total RNA-Seq Kit v2 (Life Technologies) and sequenced using a S5XL sequencing system (Life Technologies) along with the Ion 540 OT2 and Chip kit (Life Technologies). Proteins were extracted and identified by liquid chromatography and mass spectrometry as described previously (Pfaff et al., 2019). Briefly, proteins derived from the organic TRIzol phase of samples and were separated by SDS-PAGE. In-gel digestion was performed by trypsin, followed by purification of peptides and LC-MS/MS analyses by an EASY.nLC II coupled to a LTQ Orbitrap-Velos mass spectrometer (Thermo Fisher Scientific).

2.8.2 | FMDV inoculum sequence assembly and variant analysis

In order to create a full-length FMDV consensus sequence of the inoculum, raw reads were initially mapped against the FMDV reference FRA/1/2001 (AJ633821) using the 454 Sequencing Systems Software suite (version 3.0; Roche) with default options for quality trimming. All full or partially mapping reads were then selected for further de novo assembly using the same software. The resulting full-length FMDV sequence was annotated in Geneious (Geneious, version R10, 2018 August 1) (Kearse et al., 2012) according to the NCBI RefSeq of FMDV and uploaded to the European Nucleotide Archive (ENA) under the project accession PRJEB28325. In order to call low frequency nucleotide variants in the inoculum and in the treatment samples from different time points, the raw sequence reads were quality trimmed using Trimmomatic (Trimmomatic, version 0.36, 2018, August 1) (Bolger, Lohse, & Usadel, 2014), with a 5-base wide sliding window that cuts average qualities below 20 (phred33) and reads shorter than 50 nucleotides. Subsequently, the trimmed reads were mapped along the full-length inoculum sequence using Bowtie (Bowtie2, version 2.3.4.1, 2018, August 1) in 'very-fast-local' mode. Duplicated reads were marked and removed from the resulting alignments using SAMtools (SAMtools, version 1.7, 2018, August 1) and single nucleotide variants (SNV) were then called using LoFreq (LoFreq, version 2.1.3.1, 2018, August 1) (Wilm et al., 2012).

3 | RESULTS

3.1 | Primary DSP cells grew in multiple layers at the air-liquid interface

Primary cells originating from the bovine DSP were isolated and propagated in multilayers on porous membranes at the air-liquid interface. After protease digestion of epithelial tissue, filtration, removal of rapidly adhering cells, and freezing and thawing, the expression of vimentin intermediate filaments was less extensive than that of cytokeratin (data not shown). After five passages in flasks and before seeding in inserts, a larger number of cells expressed vimentin than cytokeratin (Figure 3a and b). The cells were mostly polygonal or round and expressed integrin $\alpha_V\beta_6$ to varying extent (Figure 3c). Secondary antibodies alone did not generate fluorescence at similar
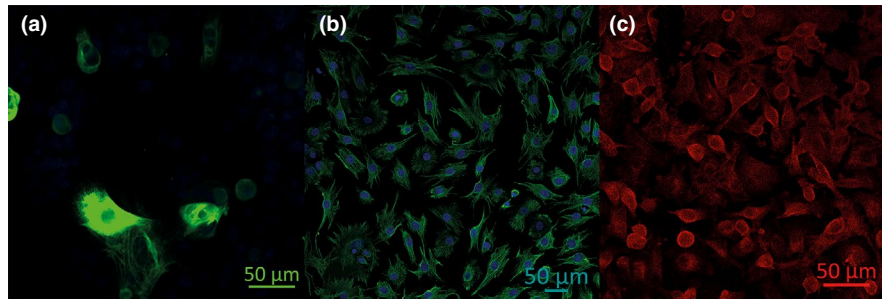
FIGURE 3 Bovine dorsal soft palate cells express cytokeratin, vimentin and integrin αVβ6 after passage in vitro. Bovine dorsal soft palate cells were isolated by protease digestion, filtration and removal of rapidly adherent cells. After freezing, thawing and three to five passages in flasks, cells were propagated in monolayers on Lab-Tek chamber slides and stained with monoclonal antibodies specific for cytokeratin (green a), vimentin (green, b) or integrin $\alpha_V\beta_6$ (red, c) and secondary antibodies conjugated with fluorescein isothiocyanate or Alexa Flour® 647. Cell nuclei were stained with DAPI (blue, a and b) and cells were visualized by confocal laser scan microscopy (in a ZEISS LSM700 microscope) [Colour figure can be viewed at wileyonlinelibrary.com]

conditions of confocal laser microscopy scanning or fluorescent microscopy (data not shown). Monolayers of the cells were infected with FMDV at an MOI of 0.01 and an almost complete CPE was observed 24 hpi (data not shown). Five days after seeding cells on inserts, the cell culture medium was removed from the upper compartment and the cells continued to grow in air. Five weeks after seeding, at the time of FMDV infection of inserts, the cells grew in multilayers and approximately 20% had a polygonal morphology and displayed tight junctions (Figure 4a and b). A subset of cells expressed cytokeratin (Figure 4c) and mRNA transcripts related to both tight junctions and cytokeratins were detected by transcriptomics (Figure 5). Whereas integrin $\alpha_V\beta_6$ expression could no longer be demonstrated by immunostaining or proteomics (data not shown), low levels of mRNA transcripts coding for the integrin chain β_6 were still detectable in most inserts (Figure 5). On the other hand, mRNA transcripts coding for the integrin chains α_V, β_1 and β_3 were abundant (Figure 5) and this was confirmed by proteomics (Figure 6).

3.2 | FMDV infection of DSP multilayers resulted in limited lysis

Foot-and-mouth disease virus (FMDV) infection of DSP multilayers in inserts resulted in limited lysis of cells in the upper cell layers, from 24 hpi to 7 dpi, as observed by light microscopy (Figure 7). At 24 hpi, infection resulted in multifocal cell detachment and loss, with foci of sparing of several layers (infection at MOI 0.01) and foci of loss of the deeper layers (infection at MOI 1), in contrast to the mock-infected membranes that did not show lysis (Figure 8). A vesicle-like structure was found in one insert at 24 hr after infection with FMDV at an MOI of 1: the multilayered epithelium was characterized by intercellular oedema and an image consistent with suprabasilar clefting (Figure 9). The CPE was more extensive at an MOI of 1, compared to 0.01 during the first 48 hr (Figure 7). Thereafter, CPE was no more observed, only cellular debris (Figure 7). The cultures seemed to have gradually recovered between 14 and 28 dpi. At 28 dpi the morphology of cells in infected and uninfected inserts did not differ (Figure 7). Sparse cytokeratin-positive cells were detected in both

infected and uninfected inserts at 28 dpi; however, by using double IHC, FMDV antigens could not be detected in these particular cells (data not shown).

3.3 | FMDV RNA and infectious FMDV persisted up to 28 dpi in DSP multilayers

Throughout the course of the experiment, cell culture washes were analysed for the presence of viral RNA by real-time RT-PCR targeting the FMDV 3D protein coding region. Whereas the internal control β-actin was detected at Ct values between 26–32 (Exp 1), 23–40 (Exp 2) and 15–39 (Exp 3), FMDV RNA was not detected in cell culture washes collected before infection, but was detected shortly after infection, at 5 hpi (Exp 2, MOI 0.01, Figure 10a), or at 2 and 4 hpi (Exp 3, MOI 1, Figure 10a). The average quantity of FMDV RNA peaked at 24 hpi (Exp 1 and 2, MOI 0.01) or 48 hpi (Exp 3, MOI 1), at almost similar levels, despite the fact that the cells originated from different animals and were infected at different MOI (Figure 10a). The peaks occurred at average Ct values of 19, 16 and 15 in experiment 1, 2 and 3, respectively. After this peak, the FMDV RNA tended to continuously decrease throughout the three experiments, although in cells infected at an MOI of 1 (Exp 3), this decrease was irregular (Figure 10a). At the termination of the experiments at 28 dpi, FMDV RNA could still be detected in cell culture medium of all infected inserts analysed (Figure 10a, $n = 8$, Ct values ranging between 25 and 28 for Exp 1 and 2, MOI 0.01 and between 22 and 27 for Exp 3, MOI 1), but not in controls ($n = 8$).

In agreement with the RT-qPCR data, live FMDV was recovered from the undiluted upper compartment wash medium by isolation on susceptible IBRS-2 cultures, from 1 dpi to 28 dpi in all experiments (Table 1). The viral titres consistently peaked on 1 dpi, at higher titres in the infections performed at an MOI of 1 (average 6.7 $\log_{10}$ TCID$_{50}$/ml, Exp 3) compared to in those performed at an MOI of 0.01 (average 6.3 $\log_{10}$ TCID$_{50}$/ml and 6.5 $\log_{10}$ TCID$_{50}$/ml in Exp 1 and 2, respectively, Figure 10b). The virus could not be titrated on 28 dpi in experiment 2 and 3 (Figure 10b), since these samples were virus negative at a dilution of 1:10, which was the

FIGURE 4 Bovine dorsal soft palate cells form multilayers at the air-liquid interface in vitro. Bovine dorsal soft palate cells were propagated on porous membrane inserts. a) Cross-section of the multilayers (double arrow) lying on PTFE membrane as visualized by light microscopy; HES stain; bar = 20 µm. b) Cross-section of the upper layer as visualized by transmission electron microscopy: tight junction (arrow) between two cells; (N: nucleus) at the upper layer; one of the cells displays apical microvilli (*); bar = 500 nm. c) Cross-section of the multilayers after antibody staining against cytokeratin (green) and visualization by a Nikon eclipse Ts2R microscope (bar = 50 µm) [Colour figure can be viewed at wileyonlinelibrary.com]
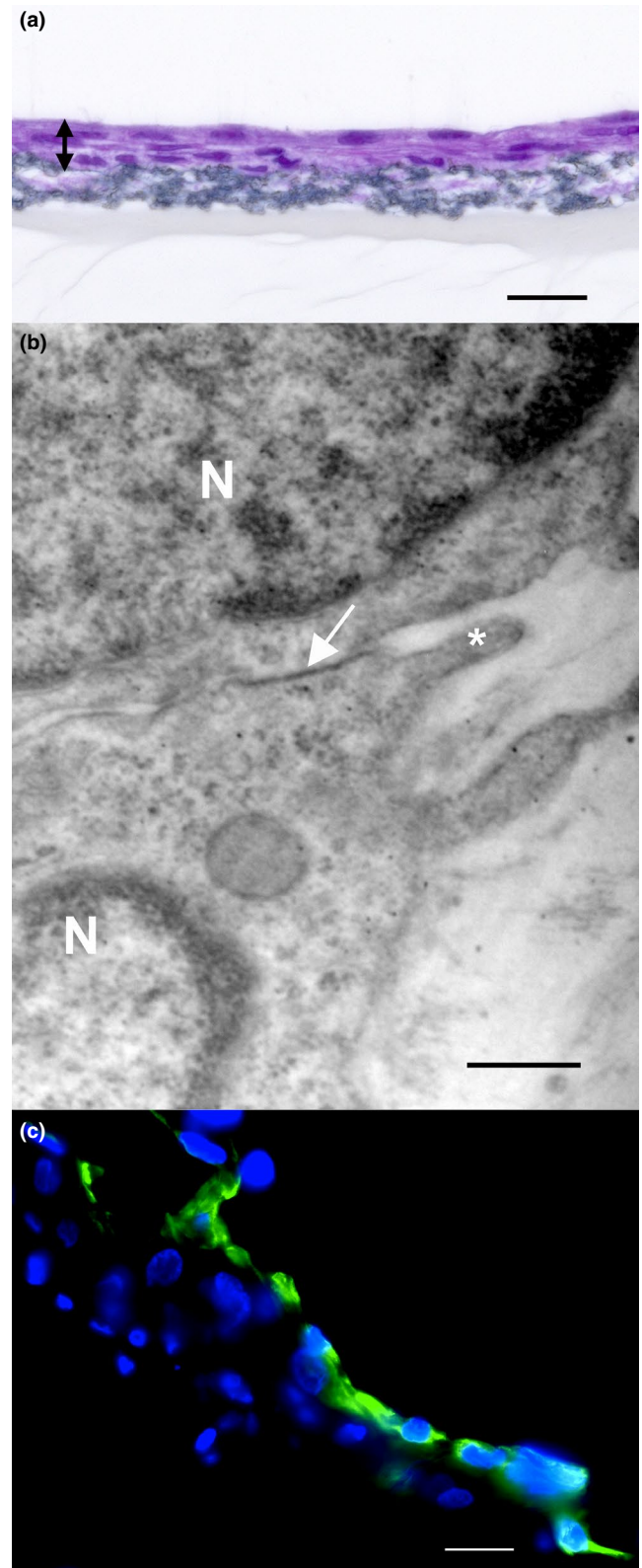
starting dilution in the viral titration assay, due to the restricted volume of wash medium. FMDV could not be isolated, neither titrated, later than 2 dpi from one insert, infected at an MOI of 1, despite presence of viral RNA until 28 dpi. This particular insert had the highest quantity of FMDV RNA on 2 dpi, compared to all inserts throughout the study. The negative samples deriving from this membrane (n = 4) were excluded from the viral titration data presented in Figure 10b, to give a better view of the titres in the remaining inserts.

3.4 | FMDV antigen persisted up to 28 dpi in a low proportion of cells

Virus antigen was detected by IHC using polyclonal antibodies, from day 1 through day 28 in the three experiments, in all inserts investigated (one per experiment and time point, as indicated in Figure 2). FMDV antigen was detected in the cytoplasm of cells at the upper, middle and lower levels of the multilayers infected at an MOI of 0.01 and at an MOI of 1 (Figure 8). The proportion of FMDV-positive cells detected by IHC using polyclonal antibodies was analysed on two sections per insert. At 24 hpi, 36% of the cells were FMDV-positive after infection at an MOI of 1, while 1 to 3% of the cells were FMDV-positive at an MOI of 0.01. At 28 dpi, the proportion of infected cells was 0.15% and 0.91% at an MOI of 0.01 (Exp 1 and Exp 2, respectively) and 2.10% at an MOI of 1 (Exp 3, Figure 11). Expression of viral non-structural protein 3D was detected by IHC in the cytoplasm of cells at all the layers at 24 hpi and 28 dpi, at an MOI of 0.01 as well as at an MOI of 1 (Figure 9). This protein was additionally detected in all the cells at the edges of the vesicle-like structure observed in one insert at 24 hpi (MOI 1; Figure 9).

3.5 | FMDV genome showed no consensus-level changes at 24 hpi

Sequencing and subsequent de novo assembly of the FMDV inoculum strain resulted in two contigs spanning the complete viral genome. Both contigs extended upstream and downstream of a long polyC stretch in the 5′UTR, whose exact length was not determined but exceeded a total number of seven cytosine nucleotides. With respect to the FMDV reference FRA/1/2001 (AJ633821), eight

Ns were introduced in order to mark this uncertainty. The genome was covered by 175,339 reads in total, of which 14,775 reads were non-duplicated (compare Table 2). In comparison to FRA/1/2001 (AJ633821), the inoculum strain FMDV O Cl 2.2 showed seven SNPs
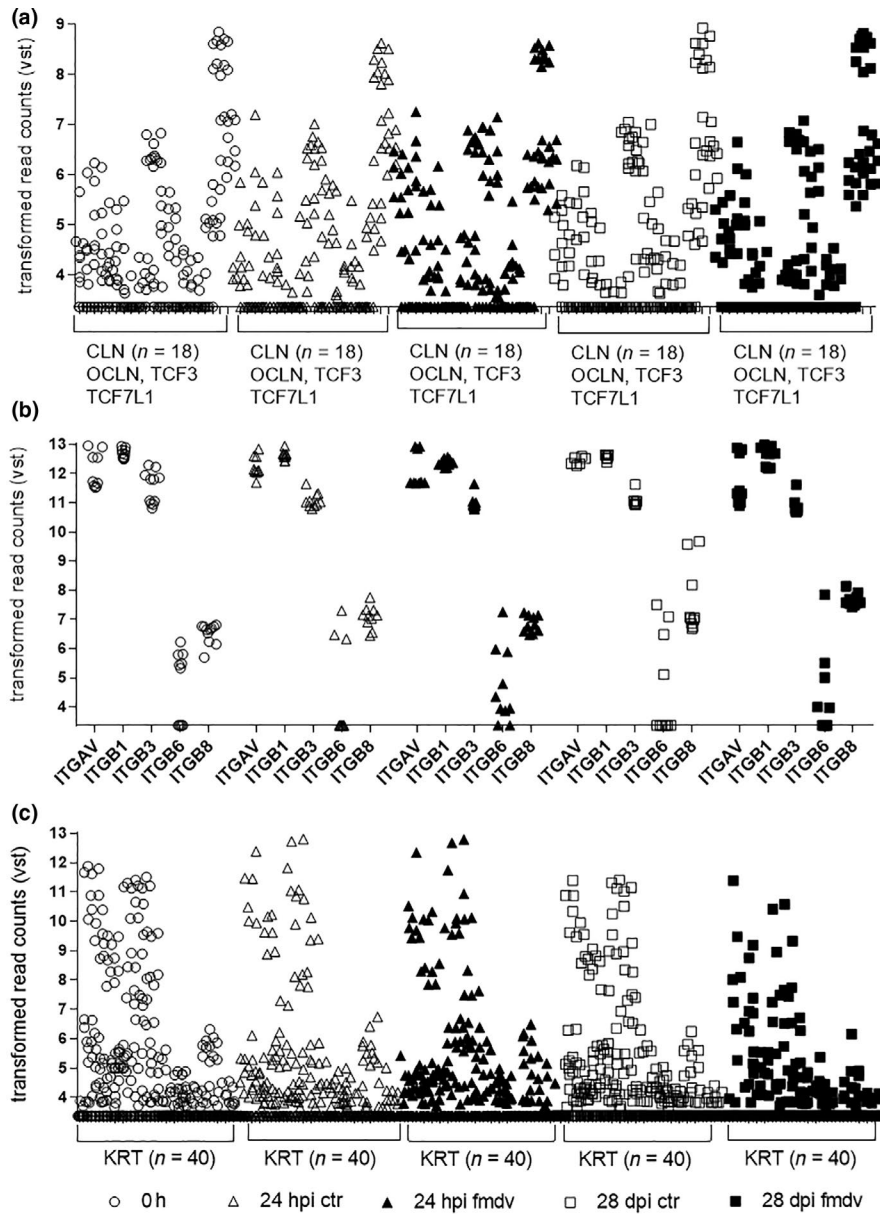
FIGURE 5 RNA transcripts related to tight junctions, FMDV receptor integrins and cytokeratins. Bovine dorsal soft palate cells were isolated and propagated in multilayers on porous membrane inserts in the air-liquid interface. After five weeks of culture, membranes were infected with FMDV at MOI 0.01 or MOI 1 or with uninfected cell lysate as placebo. Cells were harvested at indicated time points, before (0 hr, 0h) and post-infection (24 hr hpi, 28 days dpi) and total RNA was extracted. Messenger RNA was thereafter detected by RNA sequencing on the Ion S5XL system using the Ion 530 OT2 and Chip kit (Life Technologies). Gene transcripts associated with a) tight junctions (CLN, OCLN, TCF3, TCF7L1), b) FMDV-associated integrin chains (ITGAV, ITGB1, ITGB3, ITGB8) and c) cytokeratin (KRT) expression are expressed as variance stabilizing transformed (vs.t) read counts. Each data point represents a technical replicate that derived from duplicate analyses of two biological replicates
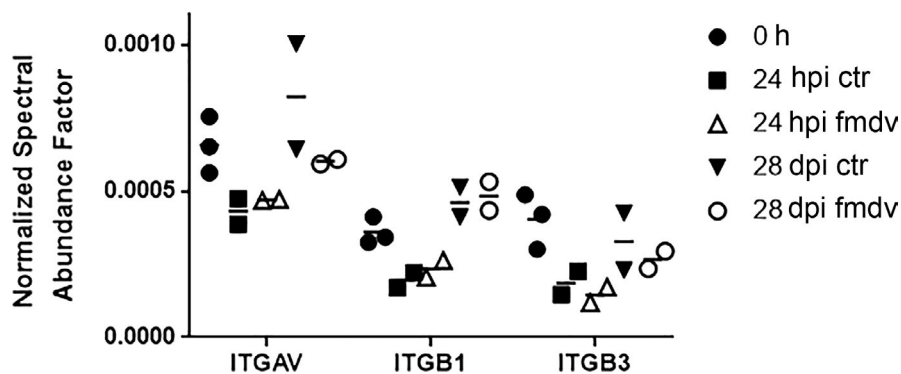

FIGURE 6 Protein expression related to FMDV receptor-associated integrins. Bovine dorsal soft palate cells were isolated and propagated in multilayers on porous membrane inserts in the air-liquid interface. After five weeks of culture, membranes were infected with FMDV at MOI 0.01 or with uninfected cell lysate as placebo. Cells were harvested at indicated time points, before and after infection. Proteins were thereafter extracted, separated by SDS-PAGE and analysed by LC-MS/MS using an EASY-nLC II coupled to a LTQ Orbitrap-Velos mass spectrometer (Thermo Fisher Scientific). ITGB6 and ITGB8 were not detected
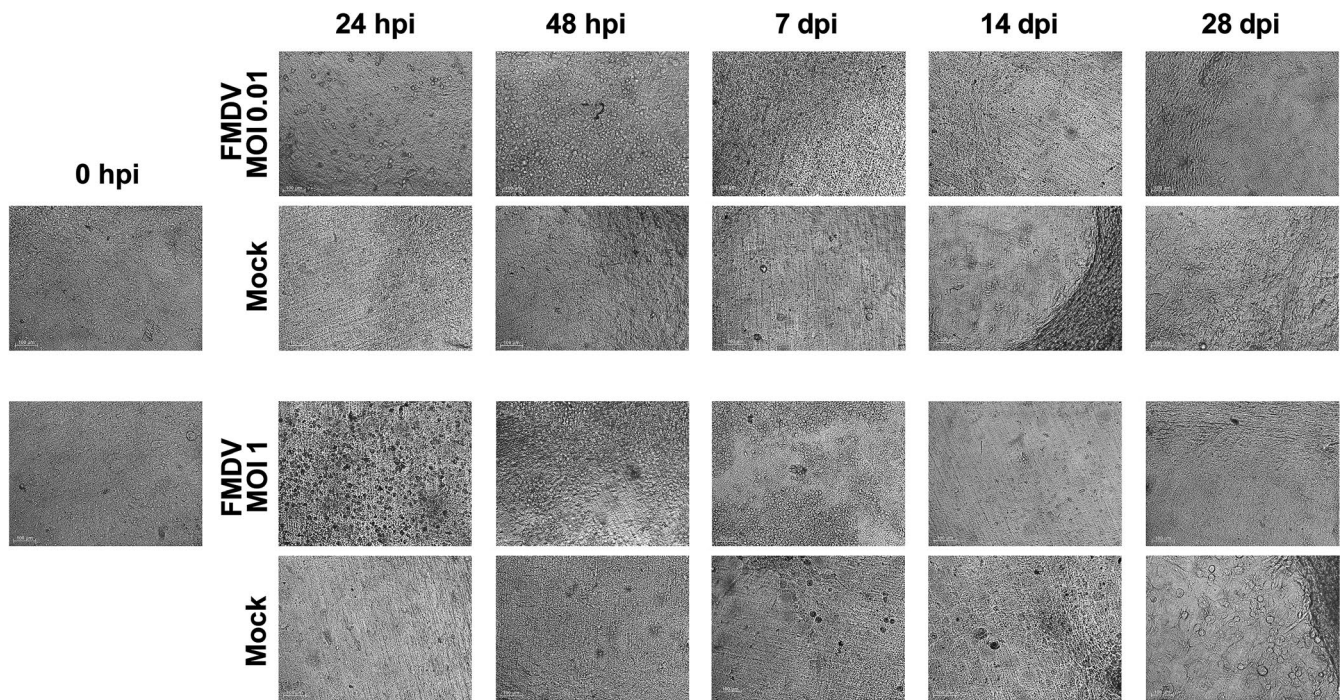
FIGURE 7 FMDV infection of multilayer cultures of bovine dorsal soft palate cells induces transient CPE in vitro. Bovine dorsal soft palate cells were isolated and propagated in multilayers on porous membrane inserts in the air-liquid interphase. After five weeks of culture, membranes were infected with FMDV at MOI 0.01 or MOI 1 or with uninfected cell lysate as placebo (Mock). A limited cytopathic effect was observed by light microscopy, at 24 hpi and up to 7 dpi, respectively, but not in mock-infected inserts. Bar = 100 µm

and a single insertion. Of these, three SNPs each were located in the 5′UTR and coding region. A single SNP and an insertion were observed in the 3′UTR. SNPs in the coding region resulted in the following amino acid substitution: A560R (1C region), E922G (1D region) and F2119I (3D region).

Reads from sequencing of FMDV O Cl 2.2 and the insert samples were mapped along the de-novo assembled FMDV O Cl 2.2 consensus sequence and SNV were called. The rate of reads matching FMDV in a certain dataset varied between <0.01% and 20.03% (Table 2) with highest and lowest rates observed within samples after 24 hpi and 28 dpi, respectively. For the inserts, no nucleotide exchanges were observed at the consensus level. Due to very low genome and overall coverage, an analysis of minor variant nucleotides below consensus level was not feasible for samples from 28 dpi. Three SNVs with variant frequencies between 0.05 and 0.06 were detected for the FMDV O Cl 2.2 that all resulted in amino acid changes in the 2C region of the polyprotein (Table 3). A single SNV at position 5,994 (T → C) that resulted in an amino acid exchange (I1355T) was also observed in three samples from the inserts taken 24 hpi at frequencies of 0.08, 0.11 and 0.13.

4 | DISCUSSION

In this work, we describe an in vitro model of FMDV persistence in multilayer cultures of DSP cells, up to 28 days post-infection. The model allows to study FMDV-specific responses of target cells, viral kinetics without influence of the adaptive immunity in vivo, or cell passage in vitro, and viral changes in absence of selective pressure from the immune system (antibodies, immune cells). The model can potentially generate complementary information on pathways and origin of some of the processes that were already identified in vivo, which have likely been based on a sum of responses from a mixture of cells, including immune cells and epithelial cells that were or were not directly exposed to the virus. Moreover, to spare animals and get a better understanding of the FMDV persistence, hypotheses raised in other in vitro models, based on cell lines or monolayers of primary cells, can be verified in the multilayer model before animal experiments are performed.

We attempted to reconstitute an epithelium with cells from the stratum basale and stratum spinosum, which together constitute the approximately nine cells deep, stratified, non-cornified, squamous epithelia in the DSP of cattle (Schley, Ward, & Zhang, 2011). The model did not reach a similar depth, but some epithelial characteristics were achieved, such as impermeability to cell culture medium from 5 days of culture on inserts, and the continuous expression of tight junctions and cytokeratin in subsets of cells.

Persistent FMDV has previously been detected post-mortem in follicle-associated epithelium in nasopharynx and the DSP, and more specifically in cytokeratin-negative and weakly positive cells in the basal cell layers (Arzt et al., 2011; Pacheco et al., 2015), as well as in highly cytokeratin-positive cells in the upper layers (Stenfeldt et al., 2016). In this study, double IHC revealed coexistence of cytokeratin-positive cells and FMDV-positive cells in the inserts at 28 dpi, but did not allow the detection of co-localization of these antigens. The
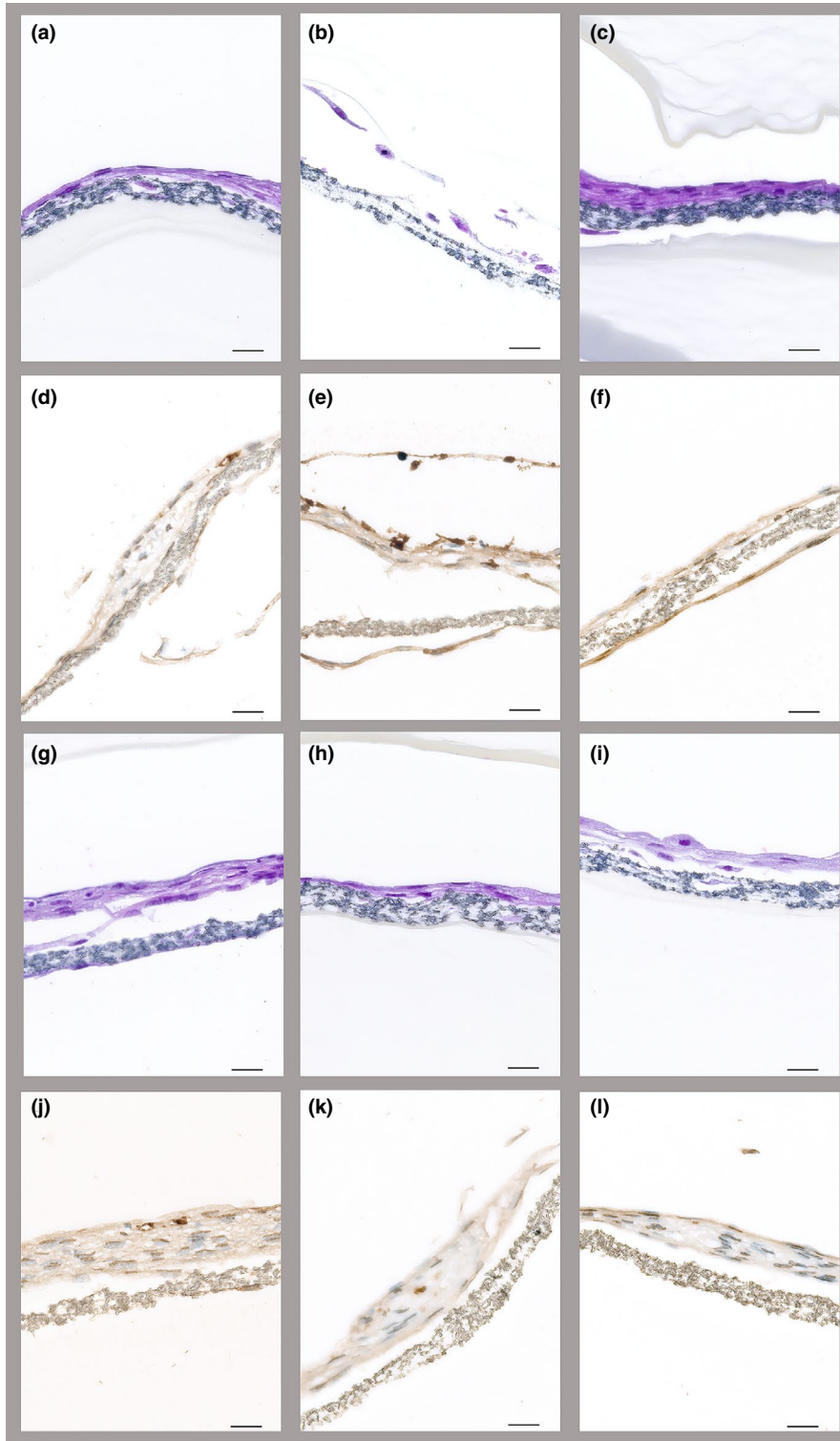
FIGURE 8 Multilayers of bovine dorsal soft palate cells show limited lysis after FMDV infection and carry persistent FMDV antigen. After five weeks of culture, dorsal soft palate multilayers were infected with FMDV at MOI 0.01 or MOI 1 or with uninfected cell lysate as placebo. At 24 hpi (a-f), infection resulted in multifocal cell detachment and loss, with foci of sparing of several layers (a, infection at MOI 0.01, Exp 2, HES stain) and foci of loss of the deeper layers (b, infection at MOI 1, Exp 3, HES stain), in contrast to the mock-infected membranes that did not show lysis (c, HES stain). The cell morphology in infected and control multilayers was similar (a-c). FMDV antigen was detected by immunohistochemistry (brown labelling) at the upper, middle and lower levels of the multilayers infected at MOI 0.01 (d) and MOI 1 (e), but not in the control multilayers (f). At 28 dpi (g-l), the infected and control multilayers were 1 to 4 cells thick with similar morphology (g, MOI 0.01, Exp 2; h, MOI 1, Exp 3; i, control; HES stain). FMDV antigen was detected by IHC (brown labelling) in a few cells at all levels of the multilayers infected at MOI 0.01 (j) and MOI 1 (k), but not in the control multilayers (l). Bar = 20 μm [Colour figure can be viewed at wileyonlinelibrary.com]

infected cells were consistently detected in all the layers on 28 dpi and cytokeratin mRNA expression persisted, albeit at lower levels compared to at the time of infection.

The majority of cells in the multilayer model expressed vimentin, but many maintained a round, flat or polygonal morphology, which suggests they were of epithelial rather than of fibroblast origin. Though vimentin was previously considered as a static fibroblast marker, both vimentin and cytokeratin can be differentially and even simultaneously expressed by the same epithelial cell (Eriksson et al., 2009; Kasper & Stosiek, 1990; Mendez, Kojima, & Goldman, 2010; Rogel et al., 2011). Vimentin expression is commonly induced when epithelial cells are cultured in vitro (Pieper et al., 1992), possibly during cell passage, because injured epithelial cells undergo epithelial to mesenchymal transition in vivo, in a process that may be reversed
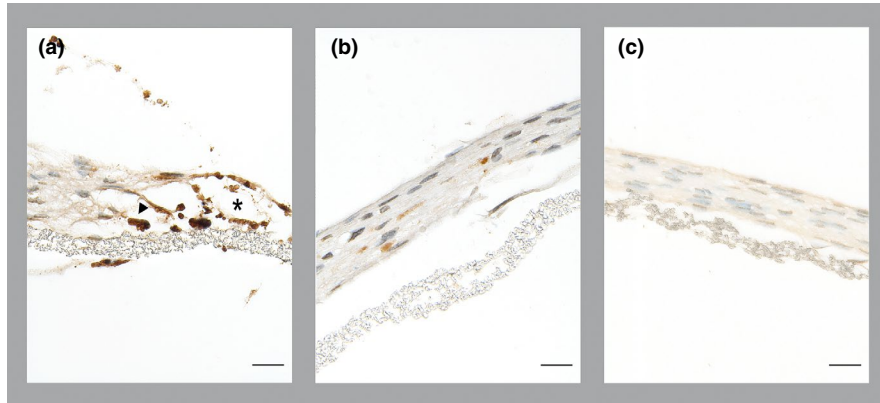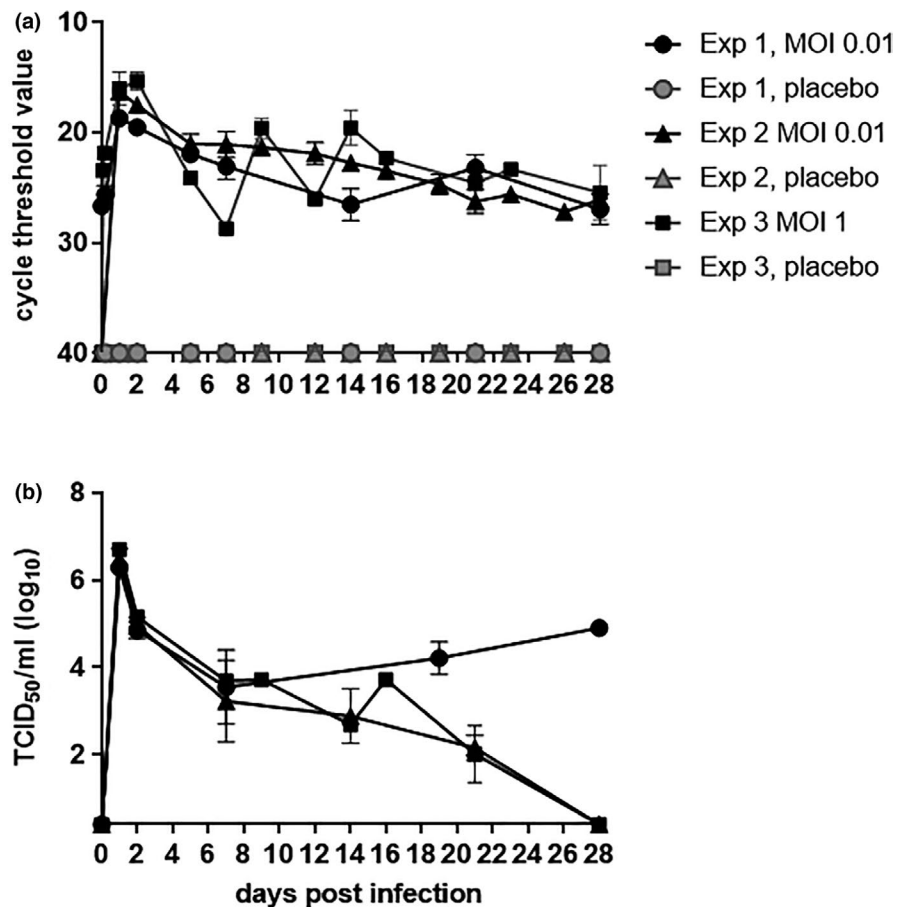
FIGURE 9 Expression of FMDV non-structural protein 3D in multilayers of bovine dorsal soft palate after FMDV infection. Expression of viral non-structural protein 3D was detected by immunohistochemistry in the cytoplasm of cells after infection at an MOI of 1 at 24 hpi (a) and at 28 dpi (b) but not in the control multilayers (c). A vesicle-like structure with intercellular oedema (star) and an image consistent with suprabasilar clefting (arrowhead) was detected 24h after infection at an MOI of 1; the basal cells and the other cells at the edges of the cleft expressed viral 3D. Bar = 20 μm [Colour figure can be viewed at wileyonlinelibrary.com]

FIGURE 10 FMDV RNA and live FMDV can be recovered from persistently infected bovine dorsal soft palate cells that are propagated in vitro. Bovine dorsal soft palate cells were isolated and propagated in multilayers on porous membrane inserts in the air-liquid interface. After five weeks of culture, membranes were infected with FMDV at MOI 0.01 (a) or MOI 1 (b) or with uninfected cell lysate as placebo. The cells were repeatedly washed with cell culture medium. The wash from 1–6 inserts, collected at indicated time points, was analysed for presence of the 3D polymerase coding region of FMDV RNA by RT-qPCR or was serially diluted from 1:10 and inoculated on susceptible IBRS-2 cultures. After three days of incubation, cells were fixed, stained with methylene blue and the $TCID_{50}$ calculated based on CPE

(Mendez et al., 2010; Rogel et al., 2011). In the present model, fibroblast contamination was decreased or avoided by removal of rapidly adhering cells, elimination of cultures that contained elongated cells and the addition of hepatocyte growth factor that is mitogenic to keratinocytes and inhibits fibrosis (Marchand-Adam et al., 2006).

Following infection with FMDV at an MOI of 0.01 or 1, the multilayer DSP cells showed only limited CPE and rapid recovery. Only one vesicle-like structure was found in one insert at 24 hr after infection with FMDV at an MOI of 1, with an image consistent with suprabasilar clefting described in the early vesicles in bovine (Arzt, Gregg, Clavijo, & Rodriguez, 2009). This is in agreement with the observed absence of lesions and the very restricted FMDV replication that occurs in the DSP in vivo (Stenfeldt & Belsham, 2012; Zhang & Alexandersen, 2004). It has been suggested that the low

TABLE 1 Isolation of FMDV during long-term culture of bovine dorsal soft palate cells on porous membrane inserts in the air-liquid interphase

dpi[a]	Exp 1[b] MOI 0.01	Exp 2[b] MOI 0.01	Exp 3[b] MOI 1
0	0/1	0/3	0/3
1	2/2	4/4	3/3
2	2/2	4/4	3/3
5	2/2	2/2	0/1
7	2/2	4/4	0/1
9	NA	4/4	1/2
12	NA	4/4	1/1
14	2/2	4/4	2/2
16	NA	4/4	1/1
19	NA	3/4	1/1
21	2/2	3/4	1/3
23	NA	2/3	1/1
26	NA	1/3	0/1
28	2/2	3/3	1/3

[a]Bovine soft palate cells were propagated in multilayers in vitro, on porous membrane inserts in the air-liquid interface and were infected with FMDV O Cl2.2at an MOI of 0.01 (experiment 1 and 2), or 1 (experiment 3) 0 days post-infection (dpi).

[b]Cell culture medium from the inserts was analysed for the presence of live FMDV by isolation on IBRS-2. The IBRS-2 cells were monitored for cytopathic effect for 48 hr and immunofluorescent detection was performed using monoclonal antibodies raised against the capsid protein VP2 of FMDV type O (mAb 13G11), as described in Kopliku et al. (2015).

FIGURE 11 The proportion of bovine dorsal soft palate cells that carry persistent FMDV antigen is low. Multilayers of dorsal soft palate cells were infected with FMDV at an MOI of 0.01 (Exp 1 and 2) or at an MOI of 1 (Exp 3). The proportion of FMDV-positive cells was analysed by immunohistochemistry and cell counting, on two sections per insert. At 24 hpi, 36% of the cells were FMDV-positive after infection at an MOI of 1, while 1 to 3% of the cells were FMDV-positive at an MOI of 0,01. At 28 dpi and regardless of MOI, less than 3% off cells were infected

susceptibility to infection in this tissue, in comparison with, for example the lung, is due to low expression of both the FMDV receptor integrin $\alpha_V\beta_6$ (Giorgakoudi et al., 2015; Monaghan et al., 2005) and of TNF superfamily genes that are linked to apoptosis and necrosis (Zhu et al., 2013). Accordingly, whereas integrin $\alpha_V\beta_6$ was expressed by subsets of DSP cells after isolation, and these cells were susceptible to FMDV-mediated lysis, integrin $\alpha_V\beta_6$ expression could not be detected in the multilayers that were more resistant. Nevertheless, the multilayer cells were also infected, maybe through integrins $\alpha_V\beta_1$,
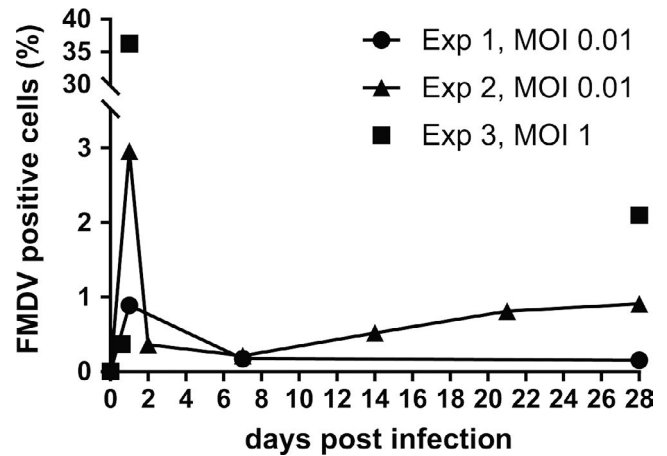
$\alpha_V\beta_3$, $\alpha_V\beta_6$, $\alpha_V\beta_8$ (O'Donnell et al., 2014; Wang, Wang, Shang, Zhang, & Liu, 2015), heparane sulphate (Bai et al., 2014; Jackson et al., 1996), or other proteins that have not yet been characterized (Baranowski et al., 2000). Our model probably mirror what happens naturally but since the virus had been passed in cell culture, it cannot be excluded that the receptor use had changed compared to that of the parental strain (Baranowski et al., 1998; O'Donnell et al., 2014).

The virus replication data based on isolations and RT-qPCR on washes of the DSP cells, correlated well with the CPE. Virus replication was observed soon after infection and declined to a minimum at 28 dpi. Whereas FMDV RNA was detected in all infected inserts throughout the experiment, live virus was not detected consistently in all inserts analysed. The detection of live virus was more successful at the lower MOI (MOI 0.01) after 2 dpi, maybe because at the higher MOI (MOI 1), more cells had been lysed and free virus

TABLE 2 Reads matching the FMDV genome from the sequencing of the inoculum and samples from inserts 24 hpi and 28 dpi

Sample	Total reads	Reads mapped to FMDV O Cl 2.2	Rate	Unique Reads mapped to FMDV O Cl 2.2	Average coverage	Genome coverage
FMDV O Cl 2.2 (lib02533)	1.389.330	175,339	12.62%	14.775	405.4	100%
24 hpi, male, Exp 1, I (lib02361)	13.634.337	134,098	0.98%	5.976	82.0	100%
24 hpi, male, Exp 1, II (lib02345)	12.959.531	286,935	2.21%	6.735	93.8	100%
24 hpi, female, Exp 2, I (lib02451)	14.295.264	2,511,451	17.57%	8.531	131.3	100%
24 hpi, female, Exp 2, II (lib02452)	15.724.713	3,149,451	20.03%	8.540	135.3	100%
28 dpi, male, Exp 1, I (lib02347)	10.782.214	2,201	0.02%	776	8.8	99.2%
28 dpi, male, Exp 1, II (lib02349)	12.869.179	975	0.01%	392	4.2	90.3%
28 dpi, female, Exp 2, I (lib02455)	13.745.858	875	0.01%	241	3.3	78.2%
28 dpi, female, Exp 2, II (lib02456)	15.570.465	468	<0.01%	127	1.6	50%

TABLE 3 Minor nucleotide variants detected in the inoculum used for infection and samples from cell inserts after 24 hpi

Sample	Genome position	Frequency	Unique depth	Change	CDS position	AA change	Region
FMDV O Cl 2.2 (lib02533)	5,399	0.056047	339	G -> A	1,193	Ala -> Thr	2C
	5,407	0.061224	343	T -> C	1,195	Leu -> Pro	2C
	5,994	0.064182	483	T -> C	1,355	Ile -> Thr	2C
24 hpi, male, Exp 1, I (lib02361)	5,994	0.081081	74	T -> C	1,355	Ile -> Thr	2C
24 hpi, male, Exp 1, II (lib02345)	5,994	0.112360	89	T -> C	1,355	Ile -> Thr	2C
24 hpi, female, Exp 2, I (lib02451)							
24 hpi, female, Exp 2, II (lib02452)	5,994	0.130000	100	T -> C	1,355	Ile -> Thr	2C

had been removed by washing. The discrepancy between virus isolation and RT-qPCR late in the infection might be explained by a production of defective virus particles, or by inhibition of live virus, by molecules such as type I interferons, defensins, cathelicidins or interfering RNA (Stenfeldt, Arzt, et al., 2017). As described by Pfaff et al. in a joint publication on the transcriptome of this model, such innate responses were activated (Pfaff et al., 2019), although they were probably modulated by the virus, based on findings in vivo (Stenfeldt et al., 2016; Zhu et al., 2013).

The declining quantity of FMDV over time, which is also observed in vivo, suggests that the virus can infect and replicate at a low level, but not indefinitely, not even in the absence of the adaptive immune responses that are important to clear virus (Maddur et al., 2009; Stenfeldt, Eschbaumer, et al., 2017). The persistent FMDV infection thus appears as a chronic infection that is self-limiting. The multilayer model can be kept for at least three months and long-term persistence could thereby be further investigated in future studies.

Besides being associated with host factors, persistence may also rely on genetic and antigenic changes in the virus. In our model, no such changes were apparent. The consensus sequence of the virus was consistent throughout the acute and persistent phases of infection and we did not observe an accumulation of minor nucleotide variants below the consensus. The use of a viral clone might have favoured this lack of variation, although generation of mutations was previously demonstrated with plaque-purified virus (Huang, Li, Fang, & Zheng, 2011; de la Torre et al., 1988). Similarly, non-synonymous nucleotide exchanges occur within and between hosts during natural infections (Cottam, King, Wilson, Paton, & Haydon, 2009; Morelli et al., 2013) and are likely driven by selective pressure from the adaptive immune system (Gebauer et al., 1988). It has been suggested that such changes could allow viral subpopulations to escape clearance by the immune system and facilitate persistent infection (Horsington & Zhang, 2007). Previous studies have described persistence-associated amino acid substitutions in serotype O viruses (Horsington & Zhang, 2007; Pauszek et al., 2017; Ramirez-Carvajal et al., 2018), but neither these nor any other viral determinants of persistence were identified in this study.

In conclusion, this new model of bovine DSP allows long-term culture without disruption of cells and mimics the in vivo conditions, in the way that soft palate cells grow in multilayers and are in contact with air. The model will make it possible to get a better understanding of the mechanisms underlying FMDV persistence in order to develop ways to control this infection and to improve its diagnosis.

CONFLICT OF INTEREST

The authors declare that they have no conflict of interest.

ETHICAL STATEMENT

The authors confirm that the ethical policies of the journal, as noted on the journal's author guidelines page, have been adhered to. No ethical approval was required as the samples were collected after commercial slaughter.

ORCID

Sara Hägglund https://orcid.org/0000-0002-6983-5722

Martin Beer https://orcid.org/0000-0002-0598-5254

Sandra Blaise-Boisseau https://orcid.org/0000-0002-8812-2023

Jean François Valarcher https://orcid.org/0000-0002-8564-5603

REFERENCES

Alexandersen, S., Quan, M., Murphy, C., Knight, J., & Zhang, Z. (2003). Studies of quantitative parameters of virus excretion and transmission in pigs and cattle experimentally infected with foot-and-mouth disease virus. *Journal of Comparative Pathology*, *129*(4), 268–282. https://doi.org/10.1016/S0021-9975(03)00045-8

Alexandersen, S., Zhang, Z., & Donaldson, A. I. (2002). Aspects of the persistence of foot-and-mouth disease virus in animals–the carrier problem. *Microbes and Infection*, *4*(10), 1099–1110. https://doi.org/10.1016/S1286-4579(02)01634-9

Arzt, J., Belsham, G. J., Lohse, L., Botner, A., & Stenfeldt, C. (2018). Transmission of foot-and-mouth disease from persistently infected carrier cattle to naive cattle via transfer of oropharyngeal fluid. *mSphere*, *3*(5), 1–12. https://doi.org/10.1128/mSphere.00365-18

Arzt, J., Gregg, D. A., Clavijo, A., & Rodriguez, L. L. (2009). Optimization of immunohistochemical and fluorescent antibody techniques for localization of Foot-and-mouth disease virus in animal tissues. *Journal of Veterinary Diagnostic Investigation*, *21*(6), 779–792. https://doi.org/10.1177/104063870902100604

Arzt, J., Juleff, N., Zhang, Z., & Rodriguez, L. L. (2011). The pathogenesis of foot-and-mouth disease I: Viral pathways in cattle. *Transboundary and Emerging Diseases*, *58*(4), 291–304. https://doi.org/10.1111/j.1865-1682.2011.01204.x

Bai, X., Bao, H., Li, P., Wei, W., Zhang, M., Sun, P. U., ... Liu, Z. (2014). Effects of two amino acid substitutions in the capsid proteins on the interaction of two cell-adapted PanAsia-1 strains of foot-and-mouth disease virus serotype O with heparan sulfate receptor. *Virology Journal*, *11*, 132. https://doi.org/10.1186/1743-422X-11-132

Baranowski, E., Ruiz-Jarabo, C. M., Sevilla, N., Andreu, D., Beck, E., & Domingo, E. (2000). Cell recognition by foot-and-mouth disease virus that lacks the RGD integrin-binding motif: Flexibility in aphthovirus receptor usage. *Journal of Virology*, *74*(4), 1641–1647. https://doi.org/10.1128/jvi.74.4.1641-1647.2000

Baranowski, E., Sevilla, N., Verdaguer, N., Ruiz-Jarabo, C. M., Beck, E., & Domingo, E. (1998). Multiple virulence determinants of foot-and-mouth disease virus in cell culture. *Journal of Virology*, *72*(8), 6362–6372.

Bertram, M. R., Vu, L. T., Pauszek, S. J., Brito, B. P., Hartwig, E. J., Smoliga, G. R., ... Arzt, J. (2018). Lack of transmission of foot-and-mouth disease virus from persistently infected cattle to naïve cattle under field conditions in Vietnam. *Frontiers in Veterinary Science*, *5*, 174. https://doi.org/10.3389/fvets.2018.00174

Bolger, A. M., Lohse, M., & Usadel, B. (2014). Trimmomatic: A flexible trimmer for Illumina sequence data. *Bioinformatics*, *30*(15), 2114–2120. https://doi.org/10.1093/bioinformatics/btu170

Bowtie2. (version 2.3.4.1, 2018, August 1). Retrieved from http://bowtie-bio.sourceforge.net/bowtie2/index.shtml.

Bravo de Rueda, C., de Jong, M. C., Eble, P. L., & Dekker, A. (2015). Quantification of transmission of foot-and-mouth disease virus caused by an environment contaminated with secretions and excretions from infected calves. *Veterinary Research*, *46*, 43. https://doi.org/10.1186/s13567-015-0156-5

Bronsvoort, B. M. D. C., Handel, I. G., Nfon, C. K., Sørensen, K.-J., Malirat, V., Bergmann, I., ... Morgan, K. L. (2016). Redefining the "carrier" state for foot-and-mouth disease from the dynamics of virus persistence in endemically affected cattle populations. *Scientific Reports*, *6*, 29059. https://doi.org/10.1038/srep29059

Burman, A., Clark, S., Abrescia, N. G., Fry, E. E., Stuart, D. I., & Jackson, T. (2006). Specificity of the VP1 GH loop of Foot-and-Mouth Disease virus for alphav integrins. *Journal of Virology*, *80*(19), 9798–9810. https://doi.org/10.1128/JVI.00577-06

Cottam, E. M., King, D. P., Wilson, A., Paton, D. J., & Haydon, D. T. (2009). Analysis of Foot-and-mouth disease virus nucleotide sequence variation within naturally infected epithelium. *Virus Research*, *140*(1–2), 199–204. https://doi.org/10.1016/j.virusres.2008.10.012

de la Torre, J. C., Davila, M., Sobrino, F., Ortin, J., & Domingo, E. (1985). Establishment of cell lines persistently infected with foot-and-mouth disease virus. *Virology*, *145*(1), 24–35. https://doi.org/10.1016/0042-6822(85)90198-9

de la Torre, J. C., Martinez-Salas, E., Diez, J., Villaverde, A., Gebauer, F., Rocha, E., ... Domingo, E. (1988). Coevolution of cells and viruses in a persistent infection of foot-and-mouth disease virus in cell culture. *Journal of Virology*, *62*(6), 2050–2058.

Eriksson, J. E., Dechat, T., Grin, B., Helfand, B., Mendez, M., Pallari, H. M., & Goldman, R. D. (2009). Introducing intermediate filaments: From discovery to disease. *Journal of Clinical Investigation*, *119*(7), 1763–1771. https://doi.org/10.1172/JCI38339

Eschbaumer, M., Stenfeldt, C., Rekant, S. I., Pacheco, J. M., Hartwig, E. J., Smoliga, G. R., ... Arzt, J. (2016). Systemic immune response and virus persistence after foot-and-mouth disease virus infection of naive cattle and cattle vaccinated with a homologous adenovirus-vectored vaccine. *BMC Veterinary Research*, *12*, 205. https://doi.org/10.1186/s12917-016-0838-x

Gebauer, F., de la Torre, J. C., Gomes, I., Mateu, M. G., Barahona, H., Tiraboschi, B., ... Domingo, E. (1988). Rapid selection of genetic and antigenic variants of foot-and-mouth disease virus during persistence in cattle. *Journal of Virology*, *62*(6), 2041–2049.

Geneious. (version R10, 2018 August 1). Retrieved from http://www.geneious.com.

Giorgakoudi, K., Gubbins, S., Ward, J., Juleff, N., Zhang, Z., & Schley, D. (2015). Using mathematical modelling to explore hypotheses about the role of bovine epithelium structure in foot-and-mouth disease virus-induced cell lysis. *PLoS ONE*, *10*(10), e0138571. https://doi.org/10.1371/journal.pone.0138571

Gorna, K., Relmy, A., Romey, A., Zientara, S., Blaise-Boisseau, S., & Bakkali-Kassimi, L. (2016). Establishment and validation of two duplex one-step real-time RT-PCR assays for diagnosis of foot-and-mouth disease. *Journal of Virological Methods*, *235*, 168–175. https://doi.org/10.1016/j.jviromet.2016.03.020

Horsington, J., & Zhang, Z. (2007). Consistent change in the B-C loop of VP2 observed in foot-and-mouth disease virus from persistently infected cattle: Implications for association with persistence. *Virus Research*, *125*(1), 114–118. https://doi.org/10.1016/j.virusres.2006.12.008

Huang, X., Li, Y., Fang, H., & Zheng, C. (2011). Establishment of persistent infection with foot-and-mouth disease virus in BHK-21 cells. *Virology Journal*, *8*, 169. https://doi.org/10.1186/1743-422X-8-169

Jackson, T., Ellard, F. M., Ghazaleh, R. A., Brookes, S. M., Blakemore, W. E., Corteyn, A. H., ... King, A. M. (1996). Efficient infection of cells in culture by type O foot-and-mouth disease virus requires binding to cell surface heparan sulfate. *Journal of Virology*, *70*(8), 5282–5287.

Juleff, N., Windsor, M., Reid, E., Seago, J., Zhang, Z., Monaghan, P., ... Charleston, B. (2008). Foot-and-mouth disease virus persists in the light zone of germinal centres. *PLoS ONE*, *3*(10), e3434. https://doi.org/10.1371/journal.pone.0003434

Kasper, M., & Stosiek, P. (1990). The expression of vimentin in epithelial cells from human nasal mucosa. *European Archives of Oto-Rhino-Laryngology*, *248*(1), 53–56. https://doi.org/10.1007/BF00634782

Kearse, M., Moir, R., Wilson, A., Stones-Havas, S., Cheung, M., Sturrock, S., ... Drummond, A. (2012). Geneious Basic: An integrated and extendable desktop software platform for the organization and analysis of sequence data. *Bioinformatics*, *28*(12), 1647–1649. https://doi.org/10.1093/bioinformatics/bts199

Kitching, R. P. (2002). Clinical variation in foot and mouth disease: Cattle. *Revue Scientifique Et Technique*, *21*(3), 499–504. https://doi.org/10.20506/rst.21.3.1343

Knight-Jones, T. J., & Rushton, J. (2013). The economic impacts of foot and mouth disease - what are they, how big are they and where do they

occur? *Preventive Veterinary Medicine*, *112*(3–4), 161–173. https://doi.org/10.1016/j.prevetmed.2013.07.013

Kopliku, L., Relmy, A., Romey, A., Gorna, K., Zientara, S., Bakkali-Kassimi, L., & Blaise-Boisseau, S. (2015). Establishment of persistent foot-and-mouth disease virus (FMDV) infection in MDBK cells. *Archives of Virology*, *160*(10), 2503–2516. https://doi.org/10.1007/s00705-015-2526-8

LoFreq. (version 2.1.3.1, 2018, August 1). Retrieved from http://csb5.github.io/lofreq.

Maddur, M. S., Kishore, S., Gopalakrishna, S., Singh, N., Suryanarayana, V. V., & Gajendragad, M. R. (2009). Immune response and viral persistence in Indian buffaloes (Bubalus bubalis) infected with foot-and-mouth disease virus serotype Asia 1. *Clinical and Vaccine Immunology*, *16*(12), 1832–1836. https://doi.org/10.1128/CVI.00302-09

Marchand-Adam, S., Fabre, A., Mailleux, A. A., Marchal, J., Quesnel, C., Kataoka, H., ... Crestani, B. (2006). Defect of pro-hepatocyte growth factor activation by fibroblasts in idiopathic pulmonary fibrosis. *American Journal of Respiratory and Critical Care Medicine*, *174*(1), 58–66. https://doi.org/10.1164/rccm.200507-1074OC

Maree, F., de Klerk-Lorist, L.-M., Gubbins, S., Zhang, F., Seago, J., Pérez-Martín, E., ... Juleff, N. (2016). Differential persistence of foot-and-mouth disease virus in African Buffalo Is related to virus virulence. *Journal of Virology*, *90*(10), 5132–5140. https://doi.org/10.1128/JVI.00166-16

Martin Hernandez, A. M., Carrillo, E. C., Sevilla, N., & Domingo, E. (1994). Rapid cell variation can determine the establishment of a persistent viral infection. *Proceedings of the National Academy of Sciences of the United States of America*, *91*(9), 3705–3709. https://doi.org/10.1073/pnas.91.9.3705

Mendez, M. G., Kojima, S., & Goldman, R. D. (2010). Vimentin induces changes in cell shape, motility, and adhesion during the epithelial to mesenchymal transition. *FASEB Journal*, *24*(6), 1838–1851. https://doi.org/10.1096/fj.09-151639

Monaghan, P., Gold, S., Simpson, J., Zhang, Z., Weinreb, P. H., Violette, S. M., ... Jackson, T. (2005). The alpha(v)beta6 integrin receptor for Foot-and-mouth disease virus is expressed constitutively on the epithelial cells targeted in cattle. *Journal of General Virology*, *86*(Pt 10), 2769–2780. https://doi.org/10.1099/vir.0.81172-0

Morelli, M. J., Wright, C. F., Knowles, N. J., Juleff, N., Paton, D. J., King, D. P., & Haydon, D. T. (2013). Evolution of foot-and-mouth disease virus intra-sample sequence diversity during serial transmission in bovine hosts. *Veterinary Research*, *44*, 12. https://doi.org/10.1186/1297-9716-44-12

O'Donnell, V., Pacheco, J. M., Larocco, M., Gladue, D. P., Pauszek, S. J., Smoliga, G., ... Rodriguez, L. (2014). Virus-host interactions in persistently FMDV-infected cells derived from bovine pharynx. *Virology*, *468–470*, 185–196. https://doi.org/10.1016/j.virol.2014.08.004

OIE. (2018). Chapter 2.1.8. Foot and mouth disease. In The OIE Biological Standards Commission, Adopted by the World Assembly of Delegates of the OIE, *Manual of Diagnostic*, France

OIE. (2018). *Resolutions Adopted by the World Assembly of OIE Delegates during their 86th General Session*.

Pacheco, J. M., Smoliga, G. R., O'Donnell, V., Brito, B. P., Stenfeldt, C., Rodriguez, L. L., & Arzt, J. (2015). Persistent foot-and-mouth disease virus infection in the nasopharynx of cattle; Tissue-specific distribution and local cytokine expression. *PLoS ONE*, *10*(5), e0125698. https://doi.org/10.1371/journal.pone.0125698

Parthiban, A. B., Mahapatra, M., Gubbins, S., & Parida, S. (2015). Virus excretion from foot-and-mouth disease virus carrier cattle and their potential role in causing new outbreaks. *PLoS ONE*, *10*(6), e0128815. https://doi.org/10.1371/journal.pone.0128815

Pauszek, S. J., Bertram, M. R., Vu, L. T., Hartwig, E. J., Smoliga, G. R., Brito, B., ... Arzt, J. (2017). Genome sequences of seven foot-and-mouth disease virus isolates collected from serial samples from one persistently infected carrier cow in Vietnam. *Genome Announcements*, *5*(34), 1–3. https://doi.org/10.1128/genomeA.00849-17

Pfaff, F., Hägglund, S., Zoli, M., Blaise-Boisseau, S., Laloy, E., Koethe, S., ... Eschbaumer, M. (2019). Proteogenomics uncovers critical elements of host response in bovine soft palate epithelial cells following in vitro infection with foot-and-mouth disease virus. *Viruses*, *11*(53), 1–19. https://doi.org/10.3390/v11010053

Pfaff, F., Müller, T., Freuling, C. M., Fehlner-Gardiner, C., Nadin-Davis, S., Robardet, E., ... Höper, D. (2018). In-depth genome analyses of viruses from vaccine-derived rabies cases and corresponding live-attenuated oral rabies vaccines. *Vaccine*, *37*(33), 4758–4765. https://doi.org/10.1016/j.vaccine.2018.01.083

Pieper, F. R., Van de Klundert, F. A., Raats, J. M., Henderik, J. B., Schaart, G., Ramaekers, F. C., & Bloemendal, H. (1992). Regulation of vimentin expression in cultured epithelial cells. *European Journal of Biochemistry*, *210*(2), 509–519. https://doi.org/10.1111/j.1432-1033.1992.tb17449.x

Ramirez-Carvajal, L., Pauszek, S. J., Ahmed, Z., Farooq, U., Naeem, K., Shabman, R. S., ... Rodriguez, L. L. (2018). Genetic stability of foot-and-mouth disease virus during long-term infections in natural hosts. *PLoS ONE*, *13*(2), e0190977. https://doi.org/10.1371/journal.pone.0190977

Rogel, M. R., Soni, P. N., Troken, J. R., Sitikov, A., Trejo, H. E., & Ridge, K. M. (2011). Vimentin is sufficient and required for wound repair and remodeling in alveolar epithelial cells. *The FASEB Journal*, *25*(11), 3873–3883. https://doi.org/10.1096/fj.10-170795

Rweyemamu, M., Roeder, P., Mackay, D., Sumption, K., Brownlie, J., Leforban, Y., ... Saraiva, V. (2008). Epidemiological patterns of foot-and-mouth disease worldwide. *Transboundary and Emerging Diseases*, *55*(1), 57–72. https://doi.org/10.1111/j.1865-1682.2007.01013.x

SAMtools. (version 1.7, 2018, August 1). Retrieved from http://www.htslib.org.

Schley, D., Ward, J., & Zhang, Z. (2011). Modelling foot-and-mouth disease virus dynamics in oral epithelium to help identify the determinants of lysis. *Bulletin of Mathematical Biology*, *73*(7), 1503–1528. https://doi.org/10.1007/s11538-010-9576-6

Schneider, C. A., Rasband, W. S., & Eliceiri, K. W. (2012). NIH Image to ImageJ: 25 years of image analysis. *Nature Methods*, *9*, 671–675. https://doi.org/10.1038/nmeth.2089

Stellmann, C., & Bornarel, P. (1971). Calculation tables of D 50 titres of viral suspensions and their accuracy. *Annales De L'institut Pasteur*, *121*(6), 825–833.

Stenfeldt, C., Arzt, J., Smoliga, G., LaRocco, M., Gutkoska, J., & Lawrence, P. (2017). Proof-of-concept study: Profile of circulating microRNAs in Bovine serum harvested during acute and persistent FMDV infection. *Virology Journal*, *14*(1), 71. https://doi.org/10.1186/s12985-017-0743-3

Stenfeldt, C., & Belsham, G. J. (2012). Detection of foot-and-mouth disease virus RNA in pharyngeal epithelium biopsy samples obtained from infected cattle: Investigation of possible sites of virus replication and persistence. *Veterinary Microbiology*, *154*(3–4), 230–239. https://doi.org/10.1016/j.vetmic.2011.07.007

Stenfeldt, C., Eschbaumer, M., Rekant, S. I., Pacheco, J. M., Smoliga, G. R., Hartwig, E. J., ... Arzt, J. (2016). the foot-and-mouth disease carrier state divergence in cattle. *Journal of Virology*, *90*(14), 6344–6364. https://doi.org/10.1128/JVI.00388-16

Stenfeldt, C., Eschbaumer, M., Smoliga, G. R., Rodriguez, L. L., Zhu, J., & Arzt, J. (2017). Clearance of a persistent picornavirus infection is associated with enhanced pro-apoptotic and cellular immune responses. *Scientific Reports*, *7*(1), 17800. https://doi.org/10.1038/s41598-017-18112-4

Trimmomatic. (version 0.36, 2018, August 1). Retrieved from http://www.usadellab.org/cms/?page=trimmomatic.

Wang, G., Wang, Y., Shang, Y., Zhang, Z., & Liu, X. (2015). How foot-and-mouth disease virus receptor mediates foot-and-mouth disease virus infection. *Virology Journal*, *12*, 9. https://doi.org/10.1186/s12985-015-0246-z

Wilm, A., Aw, P. P. K., Bertrand, D., Yeo, G. H. T., Ong, S. H., Wong, C. H., ... Nagarajan, N. (2012). LoFreq: A sequence-quality aware, ultra-sensitive variant caller for uncovering cell-population heterogeneity from high-throughput sequencing datasets. *Nucleic Acids Research*, *40*(22), 11189–11201. https://doi.org/10.1093/nar/gks918

Zhang, Z., & Alexandersen, S. (2004). Quantitative analysis of foot-and-mouth disease virus RNA loads in bovine tissues: Implications for the site of viral persistence. *Journal of General Virology*, *85*(Pt 9), 2567–2575. https://doi.org/10.1099/vir.0.80011-0

Zhu, J. J., Arzt, J., Puckette, M. C., Smoliga, G. R., Pacheco, J. M., & Rodriguez, L. L. (2013). Mechanisms of foot-and-mouth disease virus tropism inferred from differential tissue gene expression. *PLoS ONE*, *8*(5), e64119. https://doi.org/10.1371/journal.pone.0064119